HHS Public Access

Author manuscript

Gastroenterology. Author manuscript; available in PMC 2022 March 01.

Published in final edited form as:

Gastroenterology. 2021 March ; 160(4): 1240–1255.e3. doi:10.1053/j.gastro.2020.11.008.

A novel role of SLC26A3 in maintenance of intestinal epithelial barrier integrity

Anoop Kumar[1,2,#,$], **Shubha Priyamvada**[2,#], **Yong Ge**[3,#], **Dulari Jayawardena**[2], **Megha Singhal**[2], **Arivarasu N. Anbazhagan**[2], **Ishita Chatterjee**[2], **Aneal Dayal**[2], **Mitul Patel**[2], **Kimia Zadeh**, **Seema Saksena**[1,2], **Waddah A. Alrefai**[1,2], **Ravinder K Gill**[2], **Mojgan Zadeh**[3], **Ni Zhao**[3], **Mansour Mohamadzadeh**[3], **Pradeep K. Dudeja**[1,2,*,$]

[1]Jesse Brown VA Medical Center, University of Illinois at Chicago, Chicago, IL.

[2]Division of Gastroenterology and Hepatology, Department of Medicine, University of Illinois at Chicago, Chicago, IL.

[3]Department of Infectious Diseases and Immunology and Division of Gastroenterology, Hepatology and Nutrition, Department of Medicine, University of Florida, Gainesville, FL.

Abstract

Background: The Down Regulated in Adenoma (DRA) encoded by *SLC26A3*, a key intestinal chloride anion exchanger, has recently been identified as a novel susceptibility gene for inflammatory bowel disease (IBD). However, the mechanisms underlying the increased susceptibility to inflammation induced by the loss of DRA remain elusive.

Aims: Compromised barrier is a key event in IBD pathogenesis, the current studies were undertaken to elucidate the impact of DRA deficiency on epithelial barrier integrity and to define underlying mechanisms.

Methods: WT and DRA KO mice and crypt-derived colonoids were used as models for intestinal epithelial response. Paracellular permeability was measured using FITC (Fluorescein Isothiocyanate)-dextran flux. Immunoblotting, immunofluorescence, immunohistochemistry and

[*]**Author to whom correspondence should be addressed:** Pradeep K. Dudeja, Ph.D., Senior Research Career Scientist, Jesse Brown VA Medical Center, Professor of Physiology in Medicine, University of Illinois at Chicago, Medical Research Service (600/151), Jesse Brown VA Medical Center, 820 South Damen Avenue Chicago, IL 60612, pkdudeja@uic.edu, Tel.: (312)-569-7434 Fax. (312)-569-6487.

[#]These authors equally contributed to this work.

[$]Co-senior authors

Author contributions: Conceptualization: AK, SP, YG, DJ, MS, ANA, SK, IC, KZ, SS, WAA, RKG, MZ, NZ, MM, PKD; Data Curation: AK, SP, YG, NZ, DJ; Formal Analysis: AK, SP, YG, NZ, DJ, MS, ANA, PKD; Funding Acquisition: AK, PKD, WAA, SS, RKG,MM; Investigation: AK, SP, YG,NZ, DJ, MS, ANA, MZ, AD, MP; Methodology: AK, SP, YG, NZ, MZ, DJ, MS, ANA, AD, MP; Project Administration: AK, SP, PKD; Resources: AK, MM, PKD, WAA, SS, RKG; Software: AK, YG, NZ, DJ, ANA, MZ, MM, PKD; Supervision: AK, PKD, WAA, RKG, SS, MM, Validation: AK, YG, NZ, AD, WAA, PKD; Visualization: AK, YG, NZ, DJ, MZ,KZ, PKD; Writing (original draft): AK, YG, MM, SP; Writing (editing and revising): AK, SP, YG, DJ, MS, ANA, IC, MP, SS, WAA, RKG, MM, PKD

Conflict of interest: none

We demonstrate that DRA (key chloride transporter) plays an important role in maintaining gut barrier function as loss of the DRA gene promotes leaky gut implicated in development of IBD.

RNP-IP (Ribonucleoprotein Immunoprecipitation) assays were performed. Gut microbiome analysis was conducted to demonstrate the role of DRA deficiency on gut microbial communities.

Results: DRA KO mice exhibited an increased colonic paracellular permeability with significantly decreased levels of tight junction/adherens junction (TJ/AJ) proteins, including ZO-1, occludin and E-cadherin. A similar expression pattern of occludin and E-cadherin was observed in colonoids derived from DRA KO mice and shRNA-mediated DRA knock-down in Caco-2 cells. Microbial analysis showed gut dysbiosis in DRA KO mice. However, cohousing studies showed that dysbiosis only played a partial role in maintaining TJ protein expression. Furthermore, our results showed increased binding of RNA-binding protein CUGBP1 with occludin and E-cadherin genes in DRA KO mouse colon, suggesting post-transcriptional mechanisms play a key role in gut barrier dysfunction.

Conclusion: Our studies demonstrate a novel role of DRA in maintaining the intestinal epithelial barrier function and potential implications of its dysregulation in IBD pathogenesis.

Graphical Abstract

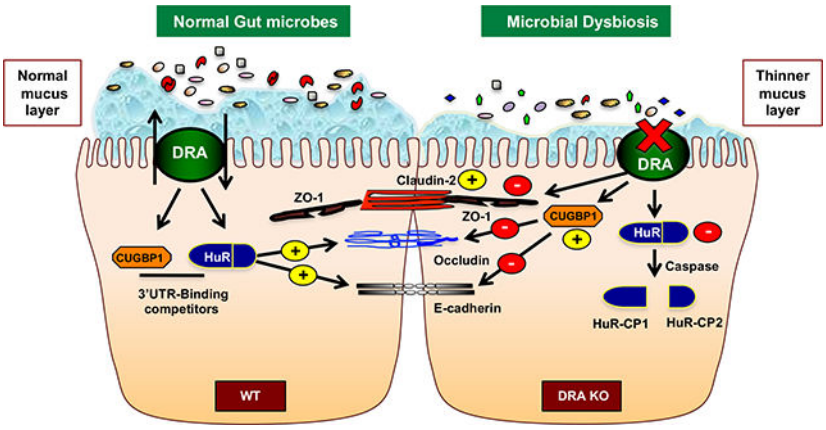

Keywords

Inflammatory bowel disease; Intestinal chloride transporter; Down regulated in adenoma; Gut microbiota

Introduction:

Inflammatory Bowel Diseases (IBD), including Crohn's disease (CD) and ulcerative colitis (UC), are chronic inflammatory intestinal disorders. The etiology of IBD is a multifactorial complex interaction that is believed to manifest from a combination of genetic, environmental, immunological and gut microbial triggers[1, 2]. Specifically, one of the key events in the pathogenesis of IBD consists of impaired epithelial barrier function that may in turn lead to increased dissemination of pathogens and their gene products (e.g., toxins) locally and peripherally in the host[3].

Previous studies have shown that changes in expression and/or distribution of tight junction (TJ) proteins lead to disrupted barrier function, observed in active CD and UC patients[3].

Further, a number of studies have shown that TJ dysregulation may be in response to cytokines or induced gut inflammation that activate distinct transcriptional and post-transcriptional mechanisms[4–6]. However, there is still a significant gap in our knowledge in understanding the molecular mechanisms involved in regulating TJ barrier function during normal homeostasis and disease manifestation. Of particular note, the intestinal ion transporters, NHE3 and DRA, have recently emerged as the key regulators of epithelial homeostasis[7, 8]. Therefore, their dysregulation may critically perturb the epithelial regulation contributing to the development and exacerbation of IBD.

DRA is the main chloride transporter involved in the intestinal vectorial NaCl absorption[1]. Inhibition of DRA expression and function has been implicated in diarrheal diseases in response to pathogen infection and gut inflammation[1]. Furthermore, mutations in the DRA gene result in congenital chloride diarrhea associated with high fecal chloride content. Additionally, DRA expression is drastically reduced in all models of colitis as well as in IBD patients[1, 9, 10]. DRA knockout mice (DRA KO mice) phenotypically display a higher IBD risk, including lack of the adherent inner mucus layer, altered proliferative homeostasis of the colonic crypts and increased susceptibility to experimental colitis[11, 12].

A recent genome wide association study (GWAS) identified SLC26A3 (DRA) as a novel IBD susceptibility gene in Japanese cohorts[13]. Similarly, a recent study performed in Chinese patients found the association of SLC26A3 polymorphism leading to decreased DRA expression with higher risk for ulcerative colitis [14]. Additionally, another recent study showed that 7 damaging variants, including SLC26A3, were located within the IBD-associated loci of Icelandic UC patients. SLC26A3 was noted to have a CADD score above 20, indicating that DRA was amongst the top 1% of deleterious variants for IBD in the human genome[15]. These data strongly suggest that DRA may not only be involved in chloride absorption but may also play an integral role in maintaining gut epithelial homeostasis. However, whether dysfunctional DRA plays an important role in the development of gut inflammation and the associated mechanisms remain unclear.

This study provides strong evidence for the novel role of DRA in maintaining intestinal epithelial integrity and identifies underlying mechanisms. By utilizing DRA KO mice, we demonstrated that the loss of DRA resulted in markedly increased colonic paracellular permeability, decreased TJ and AJ proteins and gut dysbiosis. Moreover, our studies also demonstrated that loss of DRA disrupted the TJ and AJ proteins via post-transcriptional mechanisms with no alterations in the mRNA levels. Thus, optimal DRA expression in the colonic epithelium may be integral for maintaining gut epithelial integrity and its loss in colonic epithelium could potentially contribute to the pathogenesis of IBD.

Materials and Methods:

Anti-occludin, claudin 1, 2, 3, ZO-1 and E-cadherin antibodies were obtained from Invitrogen (Carlsbad, CA) and Cell Signaling (Danvers, MA). The C-terminal amino acid sequence INTNGGLRNRVYEPVETKF of DRA was utilized to generate a DRA antibody at the Research Resources Center at the University of Illinois at Chicago (UIC)[16]. FITC-

dextran was purchased from Sigma-Aldrich (St. Louis, MO). RNA extraction and RT-PCR kits were procured from Qiagen (Valencia, CA) and Agilent (La Jolla, CA), respectively.

In vivo studies:

Prior approval for performing in vivo studies in C57BL/6 and DRA KO mice was obtained from the Institutional Animal Care Committee of Jesse Brown Veterans Affairs Medical Center and UIC. DRA KO mice were maintained on an electrolyte solution in drinking water to prevent dehydration[17]. For the first 3–4 weeks after birth and before weaning, WT mice were cage mates with DRA knockout mice and thus received the same electrolyte solution. Before sacrifice, WT mice were again maintained on the same electrolyte solution for 2 weeks in order to have an appropriate control for the experiments. The intestinal tissues were removed and the mucosa was harvested for isolating RNA and protein extraction. Additionally, the distal colons were snap frozen for immunofluorescence studies. For the cohousing studies, wild type and DRA KO mice were co-housed together for 4 weeks on electrolyte solution and the fecal matter were collected pre- and post-cohousing.

Dextran sulfate sodium (DSS) treatment:

C57BL/6J mice (male, 8 weeks of age, Jackson laboratory) were divided into two groups to either administer 3% DSS (wt/vol) (MP Biomedical, Solon, OH) in drinking water for 7 days or drinking water alone (control). Mice were euthanized and distal colonic mucosal scrapings were harvested for protein extraction.

Mouse colonoids:

Mouse colonic crypts were isolated and colonoids were cultured as previously described [16]. Briefly, each colon was dissected, rinsed with ice-cold PBS (penicillin, 100 IU/ml/ streptomycin), and divided into 1 cm sections. Tissues were incubated in PBS with 2mM EDTA at 4°C for 30 minutes on a shaker. Subsequently, tissues were treated with 54.9 mM D-sorbitol and 43.4 mM sucrose in PBS, followed by vortexing the tissues thoroughly for 1–2 minutes before filtration through a 100-μm sterile cell strainer. Filtrates were centrifuged at 150 rpm at 4°C for 10 minutes to collect the crypts, which were placed in growth factor reduced phenol-free Matrigel (BD Biosciences). Next, 60-μl droplets of Matrigel/crypt mix were placed in the center of each well of a 12-well plate in a 37°C incubator for Matrigel polymerization. Following gel polymerization, 700 μl/well of mouse organoid media (Stemcell Technologies, Vancouver, Canada) was added to the plates which were then incubated at 37°C to promote differentiation into crypt-derived colonoids that were used for experiments. The medium was changed every 2–3 days. Each experiment was repeated at least 3 times during the study.

Measuring intestinal paracellular permeability:

Mouse intestines were opened along the mesenteric border and mounted into an Easy Mount Ussing chamber system (Physiologic Instruments, San Diego, CA). Tissues were subjected to 5 ml Ringer solution (in mmol/l: 0.4 KH2PO4, 2.4 K2HPO4, 115 NaCl, 25 NaHCO3, 1.2 CaCl2, 1.2 MgCl2, 10 mannitol) on each side in a water-jacketed system maintained at 37°C. After an equilibration period of 10 min, solutions were replaced with fresh Ringer and

4 kDa FITC-dextran (Sigma) was added to the luminal side to a final concentration of 2.2 mg/mL. Intestinal permeability was determined by comparing mucosal-to-serosal flux of FITC dextran over 2 hours [18].

RNA extraction and gene expression:

RNeasy Mini Kits (Qiagen) were used for RNA extraction from mouse distal mucosal scrapings. Equivalent amounts of RNA from each sample were reverse-transcribed and amplified in a 1-step reaction using Brilliant III Ultra-fast SYBR Green QRT-PCR master mix kit (Agilent) using Mx 3000 (Agilent). The gene-specific primers for mouse DRA, occludin, ZO-1, claudins, cytokines and GAPDH have been described previously[19] and are also mentioned in Supplementary Table 1.

Western blotting:

RIPA lysis buffer (Cell Signaling, Danvers, MA) was utilized for obtaining protein lysates from the mucosa. Protein lysates were separated on 10% SDS-PAGE gels, transferred onto nitrocellulose membranes, probed with anti-TJ/AJ antibodies, followed by visualization with enhanced chemiluminescence detection reagent. Quantification of band intensity was determined using ImageJ software (NIH, Bethesda, MD).

Immunofluorescence staining of mouse colonic tissues:

Colonic tissues from WT and DRA KO mice were snap-frozen in OCT for immunostaining. Tissue sections were fixed with 4% paraformaldehyde in PBS for 15 minutes, permeabilized with 0.3% NP-40 for 5 minutes, followed by blocking with 5% normal goat serum (NGS) for 2 hr. Antibodies for the TJ/AJ proteins were incubated at 1:100 dilution in PBS with 1% NGS. After 4 washes, Alexa Fluor 594 and 488 conjugated goat anti-rabbit IgG (Invitrogen) were used for 60 min. The sections were mounted using Slowfade Gold antifade with DAPI reagent (Invitrogen), followed by imaging with a BX Fluorescent microscope (Olympus) equipped with 100X oil immersion objective.

16S rRNA gene sequencing and data analysis:

Total DNA was isolated from fecal and cecal samples using ZymoBIOMICS DNA Miniprep Kit (Zymo Research). The V4-V5 regions of 16S rRNA gene were amplified using barcoded dual-index primers [19, 2021]. PCR amplicons were purified, quantified and pooled libraries were sequenced on an Illumina Miseq instrument using a Miseq Reagent v3 kit (Illumina). The 2 × 300 bp reads were processed using QIIME 2 (v2020.2.0). Briefly, paired-reads were merged, quality trimmed and clustered into operational taxonomic units (OTUs) at 97% sequence identity. Taxonomy was assigned using the Greengenes database. OTU tables were rarefied to 45,000 sequences and the rarefied OTU tables were used to calculate alpha diversity (Shannon index) and beta diversity (weighted Unifrac distance) to determine relative abundances of taxa at multiple hierarchical levels. Linear discriminant analysis effect size (LEfSe) was performed to identify bacterial species that significantly contributed to microbiota difference by cohousing. Differentially significant taxa at each level were identified by unpaired *t*-test or Mann–Whitney *U* test.

Statistical Analysis:

The data presented are mean ± SEM of 3–6 independent experiments. Unpaired Student's *t*-test was utilized for statistical analysis. $P \leq .05$ was considered statistically significant.

Results:

Loss of DRA increases paracellular permeability in mouse colonic epithelium:

DRA KO mice are known to exhibit a significant decrease in apical Cl^-/HCO_3^- exchange activity translating to markedly higher chloride levels and water content in the stool[11]. Similarly, DRA KO mice demonstrated severe diarrhea, distended intestines and abdomen (Figures 1A and 1B). Thus, these symptoms, in addition to genotyping, were utilized in ascertaining the DRA KO phenotype. Previous studies demonstrated that DRA KO mice exhibit decreased resistance to mucosal damage induced by DSS[12]. To further examine whether the intestinal permeability is altered in DRA KO mice when compared to age-matched wild type littermates, Ussing chambers were used to measure mucosal-to-serosal FITC-dextran flux, as a surrogate for paracellular permeability in the proximal and distal colons of wild type (WT) and DRA KO mice. Here, the colons for DRA KO mice exhibited significantly higher paracellular permeability compared to those of WT mice in proximal (Figure 1C) and distal colonic regions (Figure 1D). However, no significant changes in paracellular permeability were observed in the ileal regions (Supplementary Fig 1A). These results provide novel evidence for the perturbation of epithelial barrier function under basal conditions, which may increase the susceptibility of these mice to experimental DSS induced colitis.

Loss of DRA decreases tight junction (TJ) protein expression in mouse colonic tissue:

Occludin and ZO-1 are the major transmembrane tight junction proteins that regulate the paracellular permeability to specific ions and large molecules[3]. The effect of DRA deficiency on the expression of the key TJ proteins was analyzed. There was a significant decrease in expression of occludin and ZO-1 and an increase in the expression of the pore forming protein claudin-2 in the distal colon of DRA KO mice (Figure 1E–H). Furthermore, immunostaining also demonstrated similar changes in occludin and ZO-1 expression in the distal colon of DRA KO mice, suggesting an increase in paracellular permeability (Figure 1I and 1J). In contrast, claudin-1 and 3 protein expression did not show any significant changes (Supplementary Figures 1B and C), indicating that the changes were specific to only certain TJ proteins: occludin, ZO-1 and claudin-2.

DRA KO mice exhibit decreased colonic adherens junction proteins:

In addition to TJ proteins, adherens junctions (AJ), also play an important role in maintaining the host epithelial integrity[22]. Similar to TJ proteins, there was a significant decrease in expression of the key AJ proteins, E-cadherin and β-catenin (Figure 2A and 2B). Additionally, immunostaining analysis further confirmed decreases in E-cadherin expression (Figure 2C) in the distal colon of DRA KO mice.

Gut microbiota analysis in DRA KO mice:

The gut microbiome is critical for maintenance of the intestinal epithelial barrier integrity[2324]. To investigate whether the observed reduction of intestinal permeability in DRA KO mice is related to the perturbation of gut microbiota, the bacterial communities from fecal and cecal contents derived from WT and DRA KO mice were analyzed by 16S rRNA sequencing. Bacterial diversity, as indicated by the Shannon index (measure of OTU richness and evenness), was significantly decreased in both fecal and cecal samples of DRA KO mice compared to WT mice (Figure 3A). Weighted Unifrac principal coordinate analysis (PCoA) showed a distinct difference in both cecal and fecal microbiota derived from DRA KO mice compared to WT mice (Figure 3B). In particular, the major phyla Actinobacteria was diminished in DRA KO mice compared to WT mice in fecal samples (Figure 3C). Although phylum Bacteroidetes was not significantly different between the groups, substantial differences were observed at the bacterial family level (Figures 3C and 3D). Compared to WT mice, DRA KO mice demonstrated decreased levels of Bacteroidales family S24–7 and Rikenellaceae, and significantly increased levels of Bacteroidaceae and Porphyromonadaceae in fecal and cecal samples (Figure 3D). Accordingly, *Bacteroides ovatus* and the genus *Parabacteroides* exhibited significantly higher levels in DRA KO mice compared to WT mice (Figure 3E). Within Firmicutes, Erysipelotrichaceae family members were dominant in DRA KO mice but not WT mice (Figure 3D). This was largely accounted for at the genus level by the greatly increased level of *Allobaculum* in the fecal and cecal samples of DRA KO mice (Figure 3E). Notably, DRA KO mice demonstrated significantly less butyrate-producing taxa compared to WT mice. This includes *Butyricicoccus pullicaecorum*, *Coprococcus*, *Ruminococcus*, *Odoribacter*, *Clostridium*, *Anaerostipes* and *Oscillospira* (Figure 3E and Supplemental Figure 3). Combined, these data suggest that loss of DRA significantly impacts the composition of gut microbiota in mice.

Effect of DRA deficiency on TJ/AJ proteins in mouse colonoids and Caco-2 cells:

Next, we examined TJ/AJ protein expression in colonoids generated from the DRA KO mice, as well as in Caco-2 cells where DRA was silenced by shRNA. Representative blots for colonoids (Figure 4A) and the associated densitometric analyses (Figures 4B and C) exhibited a decrease in occludin and E-cadherin expression in the colonoids generated from DRA KO mice. Additionally, shRNA-mediated-DRA-silenced Caco-2 cells also showed a decrease in occludin expression by immunoblotting (Figures 4D–F).

DRA KO mice exhibited a moderate increase in some inflammatory cytokines while mRNA expression of TJ/AJ proteins remained unchanged:

Interestingly, DRA KO mice showed a moderate increase in the pro-inflammatory cytokines CXCL1 and IL-1β (Supplementary Figures 2A and 2B). There were no significant changes observed in TNFα and IFNγ transcripts in the distal colon of DRA KO mice (Supplementary Figures 2C and 2D). With regards to TJ/AJ expression, it is noteworthy that the decreased TJ/AJ protein expression occurred only at the protein level, without any significant alterations in the transcripts of TJ/AJ (Supplementary Figures 2E, 2F, 2G, and 2H).

Role of RNA binding proteins (RBPs) in TJ/AJ protein expression in colon of DRA KO mice:

Since there was no change in TJ/AJ protein transcripts in DRA KO mice, we explored the regulation of TJ/AJ protein expression by potential post-transcriptional mechanisms. A previous report demonstrated that RNA binding proteins HuR and CUGBP1 play a key role in post-transcriptional regulation of TJ/AJ proteins[25]. Our data showed that CUGBP1 expression was significantly upregulated in the distal colon of DRA KO mice (Figure 4G). Interestingly, the protein level of intact HuR was significantly decreased while cleaved HuR (HuR CP-1) was significantly increased in DRA KO mice colon (Figure 4H). This finding is important as the cleaved product (~24kDa) has been earlier shown to change the binding ability of HuR to occludin and E-cadherin mRNA 3' UTRs[26]. Further, we tested whether increased expression of CUGBP1 leads to increased binding to the occludin and E-cadherin 3'UTRs leading to downregulation of their expression. Interestingly, our RNP-IP assay results showed significant enrichment of the binding of CUGBP1 to occludin and E-cadherin 3'UTR (Figures 4I and 4J). Taken together, these data suggest that induction of CUGBP1 and cleavage of HuR play significant roles in the mechanisms underlying disruption of barrier function in DRA KO mice.

Enhanced CUGBP1 and Cleaved HuR protein expression in DSS induced colitis:

We and others previously demonstrated that DRA[9] and tight junction proteins[27] were decreased in the distal colon of DSS-treated mice. Consistent with these reports, we observed a similar decrease in DRA (Figure 5A) and occludin expression (Figure 5B) in the distal colon of DSS treated mice. Interestingly, similar to DRA KO mice, DSS-induced colitis in mice also exhibited a marked increase in the levels of CUGBP1 (Figure 5C) and the cleaved-HuR protein (HuR CP-1). Further, there was a decrease in the level of intact HuR (Figure 5D), indicating that changes in the expression of these RNA binding proteins, as well as, the cleavage of HuR may have contributed to the downregulation of tight junction protein expression in DSS-induced colitis.

Effects of cohousing on DRA KO and WT mice:

Because mice are coprophagic, the potential for transfer of gut microbiota through the fecal-oral route is high. Thus, we used a cohousing strategy to determine whether exposure of DRA KO mice demonstrating a distinct microbial dysbiosis could impact the expression of TJ/AJ proteins involved in the barrier integrity in WT mice or vice versa. Thus, 4 weeks, post cohousing, a significant decrease in Shannon index was observed in the fecal samples of WT mice, but not in DRA KO mice, compared to fecal samples collected from the same mice before cohousing (Figure 6A). The weighted PCoA plot showed separate community clusters of the unrelated DRA KO and WT mice, with the cohoused mice forming mostly non-overlapping clusters between them (Figure 6B). This is consistent with reduced weighted Unifrac distances between cohoused DRA KO and WT mice, indicating a higher similarity than the comparison of their pre-cohoused counterparts (Figure 6C). This suggests a normalization of bacterial community structure by cohousing. Furthermore, cohousing led to a significant increase in Actinobacteria and a reduction in Bacteroidetes in both DRA KO and WT mice (Figure 6D). Next, we investigated differences in the bacterial families and

genera between cohoused DRA KO and WT mice. Here, *Parabacteroides* (Porphyromonadaceae) was more abundant in cohoused DRA KO mice compared to WT mice (Figure 6E and Supplementary Figure 3), which may suggest the limited capability of this bacterial genus to transmit horizontally. Although *Akkermansia muciniphila* (Verrucomicrobiaceae) and *Blautia producta* (Lachnospiraceae) were clearly higher in DRA KO mice than the WT mice (Figure 6E and Supplementary Figure 3), significant numbers of these bacteria were also found in WT mice during cohousing, as demonstrated by linear discriminant analysis (LDA) for effect size (LEfSe) (Figure 6F). Notably, *Allobaculum* (Erysipelotrichaceae) may potentially be acquired by WT mice from their cohoused partners (Figures 6E and 6F), while *Lactobacillus* (Lactobacillaceae), dominantly populated in the WT mice (Figure 6E), was the most distinguishing taxa enriched in cohoused DRA KO mice (Figure 6F). Cohoused WT mice, compared to their pre-cohoused controls, also had significantly more unclassified Enterococcaceae in their fecal samples, which was, by contrast, reduced in cohoused DRA KO mice (Figure 6F). Additionally, cohousing favored the propagation of some taxa in both DRA KO and WT mice, including *Staphylococcus sciuri*, *Corynebacterium stationis* and *Jeotgalicoccus psychrophilus* (Figure 6F). Taken together, these data suggest that cohousing of DRA KO and WT mice may provide opportunities for some taxa mixing and microbial community shifts toward their cohoused partners in the fecal samples.

Effect of cohousing on TJ/AJ protein expression in DRA KO mice:

The effect of cohousing on the expression of key TJ/AJ proteins was analyzed to elucidate the role of gut microbiome dysbiosis in DRA KO mice. Interestingly, our results demonstrated a slightly less, but still significant, decrease in the TJ protein expression of occludin and ZO-1 (Figure 7A–D) in distal colon of DRA KO mice. However, although the changes in the protein expression of E-cadherin also showed a decrease after cohousing, this decrease did not reach statistical significance (Figure 7A–D). Immunostaining also demonstrated similar changes in occludin, ZO-1 and E-cadherin expression in the distal colon of DRA KO mice after cohousing (Figure 7E). In addition, our results from co-housed mice also showed similar changes in RNA binding proteins CUGBP-1 and HuR expression in the DRA KO mice compared to wild type mice (Figure 7F and 7G) as seen in non-cohoused mice (Figure 4G and 4H). These data indicate that microbial dysbiosis only partly contributes to the decreases in TJ/AJ protein expression observed in DRA KO mice.

Discussion:

Impaired intestinal epithelial barrier function is one of the key risk factors in the pathogenesis of IBD [28]. However, the mechanisms underlying the dysregulation of intestinal TJ and AJ barriers under pathophysiological conditions are still evolving. Here, we present strong evidence highlighting the critical role of the chloride transporter DRA in maintaining the intestinal barrier integrity in a mouse model deficient in DRA.

DRA is a major intestinal epithelial apical membrane Cl^-/HCO_3^- exchanger that is pivotal in maintaining fluid and electrolyte absorption in the intestine. Mutations in the DRA gene in humans lead to congenital chloride diarrhea (CLD), which requires life-long supplemental

electrolyte therapy[29]. Similar to the phenotype observed in CLD patients, DRA KO mice exhibit a diarrheal phenotype[11, 12], a lack of an adherent inner mucus layer and are more prone to experimental colitis[12]. Furthermore, DRA expression is significantly reduced in animal models of infectious colitis[30] and inflammation-associated diarrhea[1, 9, 10]. Importantly, several genome wide association studies (GWAS) in Japanese, Chinese and Icelandic cohorts suggest that DRA deficiency or mutations in DRA gene are associated with higher risk for the development of ulcerative colitis[1, 1314].

Our current studies demonstrated that the DRA KO mouse colon exhibited significantly higher paracellular permeability compared to WT mice. Our data further showed a significant decrease in the expression of the TJ proteins occludin and ZO-1 and a marked increase in claudin-2 expression in DRA KO mice. In addition to alterations in TJ proteins, the AJ proteins, including E-cadherin and β-catenin were also significantly reduced in DRA KO mice. Interestingly, the maximum decrease in TJ/AJ protein expression was observed in the distal colon, which was the same region where the highest increase in paracellular permeability occurred when compared to the proximal colon and ileum in DRA KO mice. This is consistent with the finding that DRA expression is highest in the distal colon compared to other intestinal regions. The expression pattern of DRA along the length of intestine appears to parallel the barrier defect observed and, thus, may partly explain the maximum effects on TJ proteins and barrier function observed in the distal colon of DRA KO mice.

To further elucidate the direct role of DRA in gut barrier integrity, studies were also carried out with colonoids derived from DRA KO mice. Similar to our data in DRA KO mice, occludin and E-cadherin expression was significantly downregulated in DRA KO colonoids. These data indicate that DRA downregulation can also directly perturb the epithelial barrier under basal conditions, which may increase susceptibility of DRA KO mice to experimental colitis and associated diarrhea in the absence of microbial dysbiosis. In this regard, data from caco-2 cells with shRNA-mediated knock-down of DRA also showed downregulation of occludin levels, further indicating the direct involvement of DRA in maintaining TJ integrity.

To delineate the mechanism(s) underlying the changes observed in TJ/AJ proteins in DRA KO mice, we further examined the transcript levels of occludin, ZO-1, claudin-2 and E-cadherin. Interestingly, the gene expression of these proteins remained unchanged in distal colon of DRA KO mice, suggesting the involvement of post-transcriptional mechanisms. Previous studies showed that the RNA binding proteins CUGBP1 (CUG-binding protein 1) and HuR conjointly regulate the translation of occludin and E-cadherin and play a key role in TJ and AJ maintenance in IECs[25]. However, while HuR acts as a positive regulator, CUGBP1 acts as a negative regulator of TJ/AJ proteins by competing with HuR for binding to the 3'UTR of occludin and E-cadherin[22]. In our current studies, the decrease of occludin and E-cadherin protein levels in response to loss of DRA was accompanied by an increased expression in CUGBP1 and a significant decrease in intact HuR with a concomitant increase in HuR-Cleaved Protein1 (HuR CP-1). Further, increased direct binding of CUGBP-1 to occludin and E- cadherin 3'UTR as assessed by RNA-IP assay clearly showed that post transcriptional modulation of TJ protein levels by RBPs may be one of the key mechanisms

underlying barrier disruption in response to loss of DRA. We also demonstrated that DSS-colitis mice (which exhibit significant downregulation of DRA and barrier impairment), also showed a significantly increased level of CUGBP1 and a decreased level of intact HuR. However, DSS-induced colitis models are also known to exhibit histological evidence of mucosal damage and higher expression of proinflammatory cytokines, such as IL-1β, which has been shown to reduce the TJ/AJ protein expression at the mRNA level. DRA KO mice, however, did not show any histologic evidence of mucosal damage and showed significantly smaller increases in IL-1β, and did not exhibit any changes in the mRNA levels of occludin, ZO-1, claudin-2 and E-cadherin. Taken together, this suggests that the changes observed in gut permeability and TJ proteins in DRA KO mice were predominantly due to the loss of DRA and alterations in RBPs and not mediated by inflammatory mediators.

The gut microbiome plays an important role in maintaining intestinal permeability[2324]. In depth microbial analysis (down to the genus and species level) demonstrated that DRA deficiency markedly altered the gut microbial community. Specifically, DRA KO mice showed significantly reduced microbial diversity in the fecal and cecal contents. The phylum Actinobacteria was significantly decreased in the feces of DRA KO mice. A very recent study has also briefly shown microbial changes at the phylum level in DRA KO mice similar to the one reported here while being fed a special diet[31]. Interestingly, previous studies have reported that a decreased relative abundance of Actinobacteria is associated with a stress-induced increase in gut permeability[32] Also, patients with irritable bowel syndrome (IBS) show decreased abundance of Actinobacteria in stool samples[33]. The genus *Allobaculum*, which has been shown to be associated with intestinal inflammation and a leaky gut in mouse and rat models, was significantly enriched in the stool samples derived from DRA KO mice in this study[34]. Additionally, *Parabacteroides*, which has been implicated in the susceptibility of NHE3 KO mice to colitis, and *Bacteroides ovatus*, which has been implicated in the pathogenesis of IBD, were significantly enriched in fecal and cecal samples of DRA KO mice in this study[35]. Importantly, DRA KO mice exhibited significantly reduced levels of numerous butyrate-producing Clostridia bacteria, including *Butyricicoccus pullicaecorum*, *Coprococcus*, *Ruminococcus*, *Clostridium*, *Anaerostipes* and *Oscillospira*. Notably, butyrate promotes intestinal barrier function through the regulation of TJ protein assembly and expression[36, 37]. Butyrate also supports the oxygenation of intestinal epithelial cells, stabilizes the transcription factor HIF-1 and augments epithelial barrier function[38]. Thus, it is conceivable that increased intestinal permeability of DRA KO mice at least in part be due to the decreased level of butyrate-producing microbial community in the gut. It is generally accepted that cohousing normalizes the microbiota between mouse strains due to coprophagy. We consistently observed an increasingly similar composition of gut microbiota between DRA KO mice and WT mice after cohousing compared to their pre-cohoused microbiota, with bacterial taxa such as *Allobaculum* and *Lactobacillus* significantly enriched in the cohoused WT partners. Furthermore, changes in microbial composition were accompanied by the expansion of some proinflammatory bacteria such as *Facklamia* and *Staphylococcus*, which are normally suppressed by colonization resistance. Additionally, *Akkermensia muciniphila*, an important mucin-degrading intestinal bacterium, was evidently increased in WT mice through cohousing effects of DRA KO mice, which may underlie the thin mucus layer observed in DRA KO

mice[12]. Notably, after cohousing, DRA KO mice still showed a significant, decrease in the ZO-1 and occludin protein expression and significant increase in CUGBP1 and cleaved HuR levels when compared to mice that were not cohoused. However, the maximum effect of co-housing was observed on E-cadherin expression. Taken together, our data showed that optimal DRA expression plays a critical role in shaping the gut microbiota, and epithelial barrier defects in DRA KO mice may be only partly attributed to changes in the gut microbiome. Translating this mechanism to human disease, DRA deficiency, thus, may be a critical contributor to dysbiosis observed in patients with IBD.

In summary, our studies demonstrate that DRA plays a critical role in the maintenance of colonic barrier function, expression and regulation of TJ/AJ proteins, and healthy microbial community and its deficiency may lead to barrier impairment, microbial dysbiosis and development of IBD.Thus, it appears that DRA upregulation may have a dual beneficial impact in IBD by not only counteracting diarrhea, (the most debilitating symptom of IBD, through enhancing electrolyte absorption) but also correcting barrier disruption associated with IBD.

Supplementary Material

Refer to Web version on PubMed Central for supplementary material.

Acknowledgments:

Supported by Department of Veterans Affairs CDA2 Award # BX004719 (A. Kumar) VA Merit Award # BX002011 (P. K. Dudeja), VA Merit Award # BX000152 (W. A. Alrefai), VA Merit Award BX002867 (S. Saksena), and VA Senior Research Career Scientist Award # 1IK6BX005242-01 (P. K. Dudeja), Research Career Scientist Award # 1IK6BX005243-01 (W.A. Alrefai), and the NIDDK grants DK54016, DK92441 (P.K. Dudeja), DK109709 (W. A. Alrefai), DK98170 (R.K. Gill), DK109560 (M. Mohamadzadeh).

We acknowledge the help of Dr. Theodor Griggs and Mr. Nathan Calzadilla in proofreading this manuscript.

References

1. Priyamvada S, Gomes R, Gill RK, et al. Mechanisms Underlying Dysregulation of Electrolyte Absorption in Inflammatory Bowel Disease-Associated Diarrhea. Inflamm Bowel Dis 2015;21:2926–35. [PubMed: 26595422]
2. Anbazhagan AN, Priyamvada S, Alrefai WA, et al. Pathophysiology of IBD associated diarrhea. Tissue Barriers 2018:e1463897. [PubMed: 29737913]
3. Shen L, Su L, Turner JR. Mechanisms and functional implications of intestinal barrier defects. Dig Dis 2009;27:443–9. [PubMed: 19897958]
4. Al-Sadi R, Guo S, Ye D, et al. TNF-alpha modulation of intestinal epithelial tight junction barrier is regulated by ERK1/2 activation of Elk-1. Am J Pathol 2013;183:1871–1884. [PubMed: 24121020]
5. Al-Sadi R, Guo S, Ye D, et al. Mechanism of IL-1beta modulation of intestinal epithelial barrier involves p38 kinase and activating transcription factor-2 activation. J Immunol 2013;190:6596–606. [PubMed: 23656735]
6. Lee SH. Intestinal permeability regulation by tight junction: implication on inflammatory bowel diseases. Intest Res 2015;13:11–8. [PubMed: 25691839]
7. Kiela PR, Laubitz D, Larmonier CB, et al. Changes in mucosal homeostasis predispose NHE3 knockout mice to increased susceptibility to DSS-induced epithelial injury. Gastroenterology 2009;137:965–75, 975 e1–10. [PubMed: 19450596]
8. Ding X, Li D, Li M, et al. SLC26A3 (DRA) prevents TNF-alpha-induced barrier dysfunction and dextran sulfate sodium-induced acute colitis. Lab Invest 2018;98:462–476. [PubMed: 29330471]

9. Singh V, Kumar A, Raheja G, et al. Lactobacillus acidophilus attenuates downregulation of DRA function and expression in inflammatory models. Am J Physiol Gastrointest Liver Physiol 2014;307:G623–31. [PubMed: 25059823]
10. Farkas K, Yeruva S, Rakonczay Z Jr., et al. New therapeutic targets in ulcerative colitis: the importance of ion transporters in the human colon. Inflamm Bowel Dis 2011;17:884–98. [PubMed: 20722063]
11. Schweinfest CW, Spyropoulos DD, Henderson KW, et al. slc26a3 (dra)-deficient mice display chloride-losing diarrhea, enhanced colonic proliferation, and distinct up-regulation of ion transporters in the colon. J Biol Chem 2006;281:37962–71. [PubMed: 17001077]
12. Xiao F, Juric M, Li J, et al. Loss of downregulated in adenoma (DRA) impairs mucosal HCO3(−) secretion in murine ileocolonic inflammation. Inflamm Bowel Dis 2012;18:101–11. [PubMed: 21557395]
13. Asano K, Matsushita T, Umeno J, et al. A genome-wide association study identifies three new susceptibility loci for ulcerative colitis in the Japanese population. Nat Genet 2009;41:1325–9. [PubMed: 19915573]
14. Shao XX, Lin DP, Sun L, et al. Association of ulcerative colitis with solute-linked carrier family 26 member A3 gene polymorphisms and its expression in colonic tissues in Chinese patients. Int J Colorectal Dis 2018;33:1169–1172. [PubMed: 29855681]
15. Vinayaga-Pavan M, Frampton M, Pontikos N, et al. Elevation in Cell Cycle and Protein Metabolism Gene Transcription in Inactive Colonic Tissue From Icelandic Patients With Ulcerative Colitis. Inflamm Bowel Dis 2019;25:317–327. [PubMed: 30452647]
16. Kumar A, Chatterjee I, Gujral T, et al. Activation of Nuclear Factor-kappaB by Tumor Necrosis Factor in Intestinal Epithelial Cells and Mouse Intestinal Epithelia Reduces Expression of the Chloride Transporter SLC26A3. Gastroenterology 2017;153:1338–1350 e3. [PubMed: 28823863]
17. Alper SL, Stewart AK, Vandorpe DH, et al. Native and recombinant Slc26a3 (downregulated in adenoma, Dra) do not exhibit properties of 2Cl-/1HCO3-exchange. Am J Physiol Cell Physiol 2011;300:C276–86. [PubMed: 21068358]
18. Borthakur A, Priyamvada S, Kumar A, et al. A novel nutrient sensing mechanism underlies substrate-induced regulation of monocarboxylate transporter-1. Am J Physiol Gastrointest Liver Physiol 2012;303:G1126–33. [PubMed: 22982338]
19. Colliou N, Ge Y, Sahay B, et al. Commensal Propionibacterium strain UF1 mitigates intestinal inflammation via Th17 cell regulation. J Clin Invest 2017;127:3970–3986. [PubMed: 28945202]
20. Ge Y, Gong M, Colliou N, et al. Neonatal intestinal immune regulation by the commensal bacterium, P. UF1. Mucosal Immunol 2019;12:434–444. [PubMed: 30647410]
21. Ge Y, Gong M, Zadeh M, et al. Regulating colonic dendritic cells by commensal glycosylated large surface layer protein A to sustain gut homeostasis against pathogenic inflammation. Mucosal Immunol 2020;13:34–46.
22. Yu TX, Gu BL, Yan JK, et al. CUGBP1 and HuR regulate E-cadherin translation by altering recruitment of E-cadherin mRNA to processing bodies and modulate epithelial barrier function. Am J Physiol Cell Physiol 2016;310:C54–65. [PubMed: 26491048]
23. Ulluwishewa D, Anderson RC, McNabb WC, et al. Regulation of tight junction permeability by intestinal bacteria and dietary components. J Nutr 2011;141:769–76. [PubMed: 21430248]
24. Alaish SM, Smith AD, Timmons J, et al. Gut microbiota, tight junction protein expression, intestinal resistance, bacterial translocation and mortality following cholestasis depend on the genetic background of the host. Gut Microbes 2013;4:292–305. [PubMed: 23652772]
25. Yu TX, Rao JN, Zou T, et al. Competitive binding of CUGBP1 and HuR to occludin mRNA controls its translation and modulates epithelial barrier function. Mol Biol Cell 2013;24:85–99. [PubMed: 23155001]
26. Talwar S, Jin J, Carroll B, et al. Caspase-mediated cleavage of RNA-binding protein HuR regulates c-Myc protein expression after hypoxic stress. J Biol Chem 2011;286:32333–43. [PubMed: 21795698]
27. Kuo WT, Shen L, Zuo L, et al. Inflammation-induced Occludin Downregulation Limits Epithelial Apoptosis by Suppressing Caspase-3 Expression. Gastroenterology 2019;157:1323–1337. [PubMed: 31401143]

28. Michielan A, D'Inca R. Intestinal Permeability in Inflammatory Bowel Disease: Pathogenesis, Clinical Evaluation, and Therapy of Leaky Gut. Mediators Inflamm 2015;2015:628157. [PubMed: 26582965]
29. Makela S, Kere J, Holmberg C, et al. SLC26A3 mutations in congenital chloride diarrhea. Hum Mutat 2002;20:425–38. [PubMed: 12442266]
30. Borenshtein D, Schlieper KA, Rickman BH, et al. Decreased expression of colonic Slc26a3 and carbonic anhydrase iv as a cause of fatal infectious diarrhea in mice. Infect Immun 2009;77:3639–50. [PubMed: 19546193]
31. Kini A, Singh AK, Riederer B, et al. Slc26a3 deletion alters pH-microclimate, mucin biosynthesis, microbiome composition and increases the TNFalpha expression in murine colon. Acta Physiol (Oxf) 2020:e13498.
32. Sarkar A, Lehto SM, Harty S, et al. Psychobiotics and the Manipulation of Bacteria-Gut-Brain Signals. Trends Neurosci 2016;39:763–781. [PubMed: 27793434]
33. Chung CS, Chang PF, Liao CH, et al. Differences of microbiota in small bowel and faeces between irritable bowel syndrome patients and healthy subjects. Scand J Gastroenterol 2016;51:410–9. [PubMed: 26595305]
34. Alhasson F, Das S, Seth R, et al. Altered gut microbiome in a mouse model of Gulf War Illness causes neuroinflammation and intestinal injury via leaky gut and TLR4 activation. PLoS One 2017;12:e0172914. [PubMed: 28328972]
35. Saitoh S, Noda S, Aiba Y, et al. Bacteroides ovatus as the predominant commensal intestinal microbe causing a systemic antibody response in inflammatory bowel disease. Clin Diagn Lab Immunol 2002;9:54–9. [PubMed: 11777829]
36. Peng L, Li ZR, Green RS, et al. Butyrate enhances the intestinal barrier by facilitating tight junction assembly via activation of AMP-activated protein kinase in Caco-2 cell monolayers. J Nutr 2009;139:1619–25. [PubMed: 19625695]
37. Wang HB, Wang PY, Wang X, et al. Butyrate enhances intestinal epithelial barrier function via up-regulation of tight junction protein Claudin-1 transcription. Dig Dis Sci 2012;57:3126–35. [PubMed: 22684624]
38. Kelly CJ, Zheng L, Campbell EL, et al. Crosstalk between Microbiota-Derived Short-Chain Fatty Acids and Intestinal Epithelial HIF Augments Tissue Barrier Function. Cell Host Microbe 2015;17:662–71. [PubMed: 25865369]

Background:

DRA (intestinal chloride transporter) has been suggested to be a novel susceptibilty gene in IBD pathogenesis. However, the mechanisms underlying loss of DRA in increasing susceptibility to inflammation remain elusive.

New Findings:

Our data demonstrate that loss of DRA results in increased intestinal paracellular permeability, microbial dysbiosis and decrease in tight/adherens junction proteins via posttranscriptional mechanism.

Limitation:

Further studies are needed to establish if the similar mechanism is involved in patients with IBD.

Impact:

DRA upregulation may serve as a novel therapeutic approach with dual impact in IBD via beneficial effects on gut epithelial integrity as well as in counteracting IBD associated diarrhea.

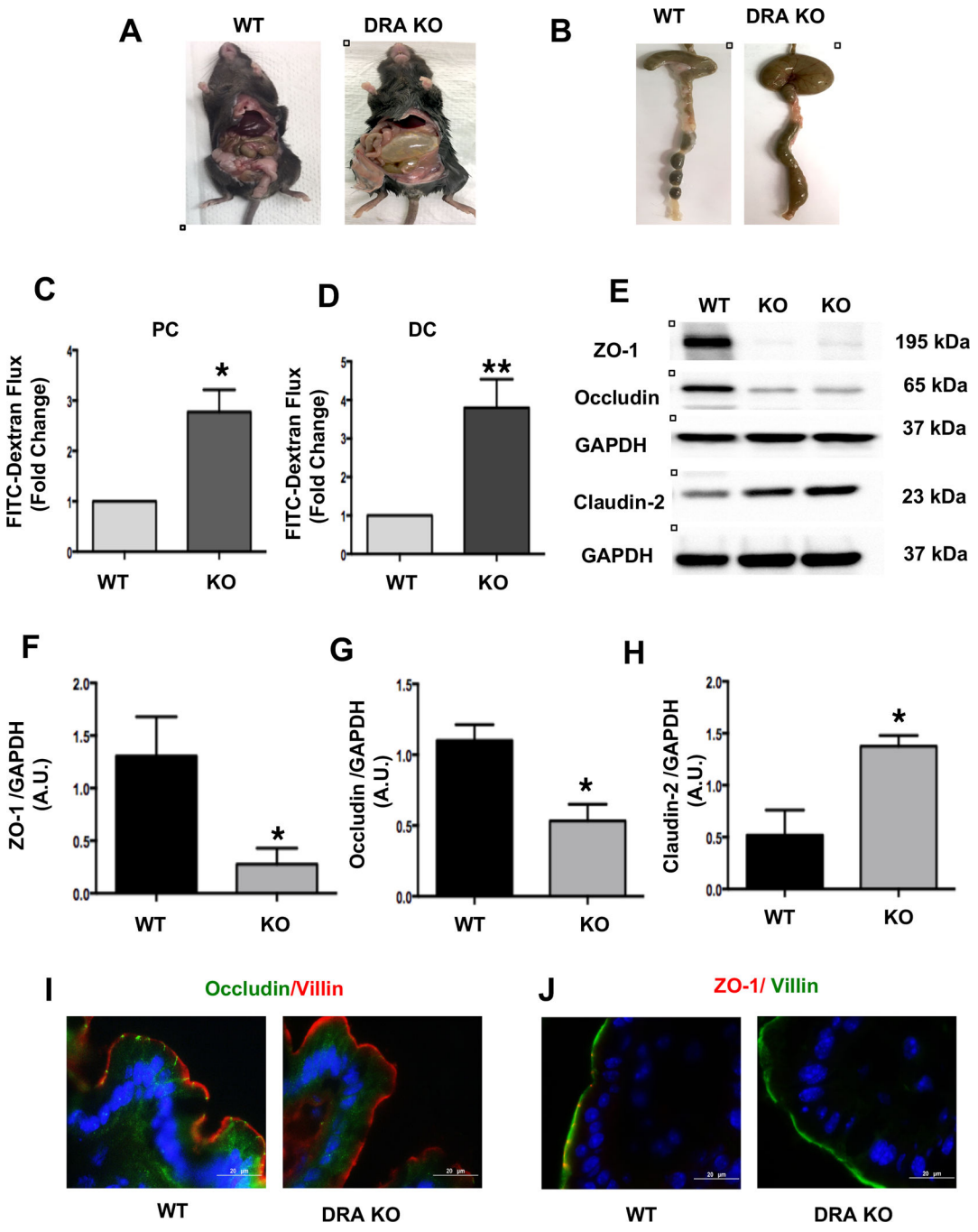

Figure 1: Loss of DRA results in increased paracellular permeability and decreased TJ protein expression in mouse colon:

DRA KO mice exhibit severe diarrhea, a distended abdomen and enlarged cecum (**Figures A and B**). DRA KO mice showed increased paracellular permeability in proximal colon (PC) and distal colon (DC) (**Figures C and D**). Intestinal permeability was determined by comparing mucosal-to-serosal flux of 4 kDa-FITC dextran (FD4) fluorescence over 120 minutes (n=3–4). Effects of DRA knockdown on protein levels of TJ components in wild type and DRA KO mice distal colon by immunoblotting are shown (**Figure E**) (n=3–6).

GAPDH was used as the internal control. Densitometric analyses of band intensities are shown (**Figures F, G, H**). Values are means ± SEM. Data was analyzed by unpaired t-test (*p <0.05 vs. wild type; **p <0.01 vs. wild type). Immunofluorescence staining of distal colon sections of wild type and DRA KO mice for occludin (green), villin (red), and DAPI (blue) (**Figure I)** and ZO-1 (red), villin (green), and DAPI (blue) (**Figure J**). Scale bar: 20 μm.

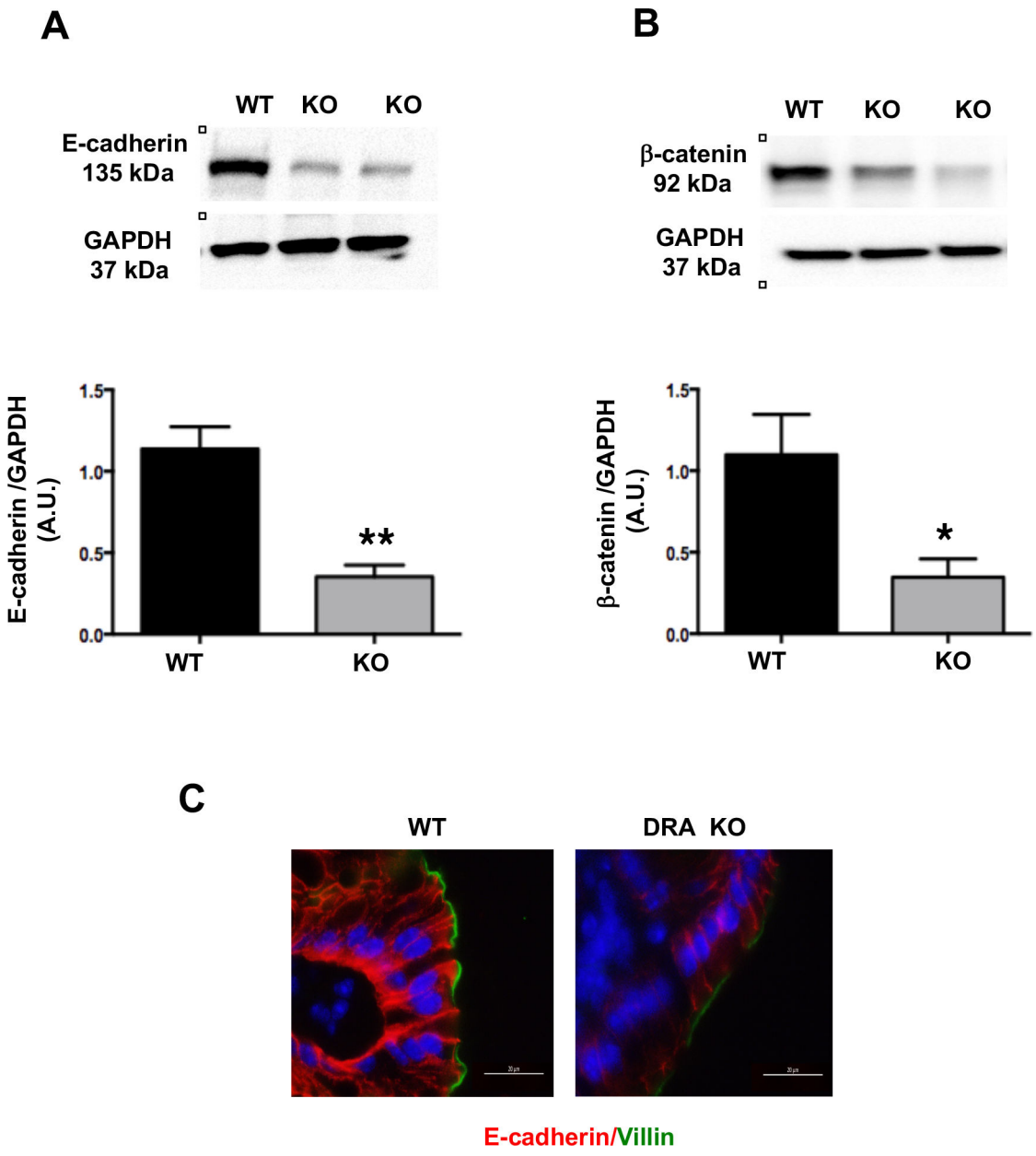

Figure 2: Loss of DRA results in decreased AJ protein expression in mouse colon:

Distal colonic mucosal lysates of wild type and DRA KO mice were subjected to SDS-PAGE and probed with E-cadherin and β-catenin antibodies. (**Figures A and B**): Densitometric analysis was performed of relative band intensities with GAPDH as internal control. Values are means ± SEM and representative blots of 3–6 independent experiments are shown. Data was analyzed by unpaired t-test (*p <0.05 vs. wild type; **p <0.01 vs. wild type). (**C**) Immunofluorescence staining of distal colonic sections of wild type and DRA KO mice for E-cadherin (red), villin (green), and DAPI (blue) is shown. Scale bar: 20 μm.

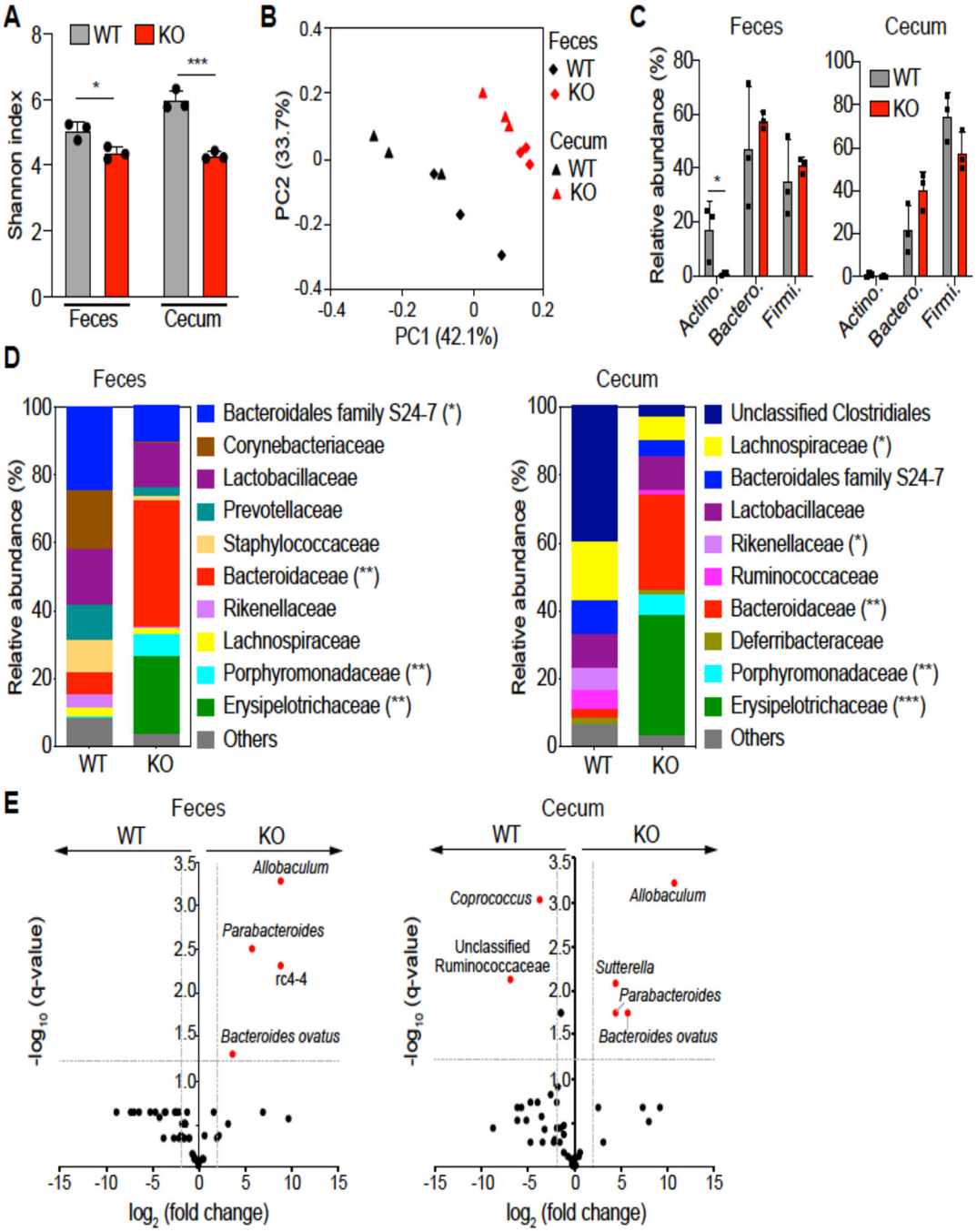

Figure 3. Loss of DRA alters gut microbial composition.

(**Figure A**) Shannon index measuring bacterial diversity by 16S rRNA sequencing in the feces and cecal contents of DRA KO and WT mice (n=3). (**Figure B**) Weighted Unifrac principal coordinate analysis (PCoA) plot separating fecal and cecal microbiota composition between DRA KO and WT mice. (**Figure C**) Top phylum abundance in the feces and cecal contents. (**Figure D**) Top family abundance of fecal and cecal microbes. Asterisks (*) indicate statistical significance between the groups of mice. (**Figure E**) Significantly different taxa between DRA KO and WT mice in fecal and cecal samples in red. The dashed

lines represent thresholds (log2 fold change > 1, FDR P <0.05). *p <0.05, **p <0.01, ***p <0.001.

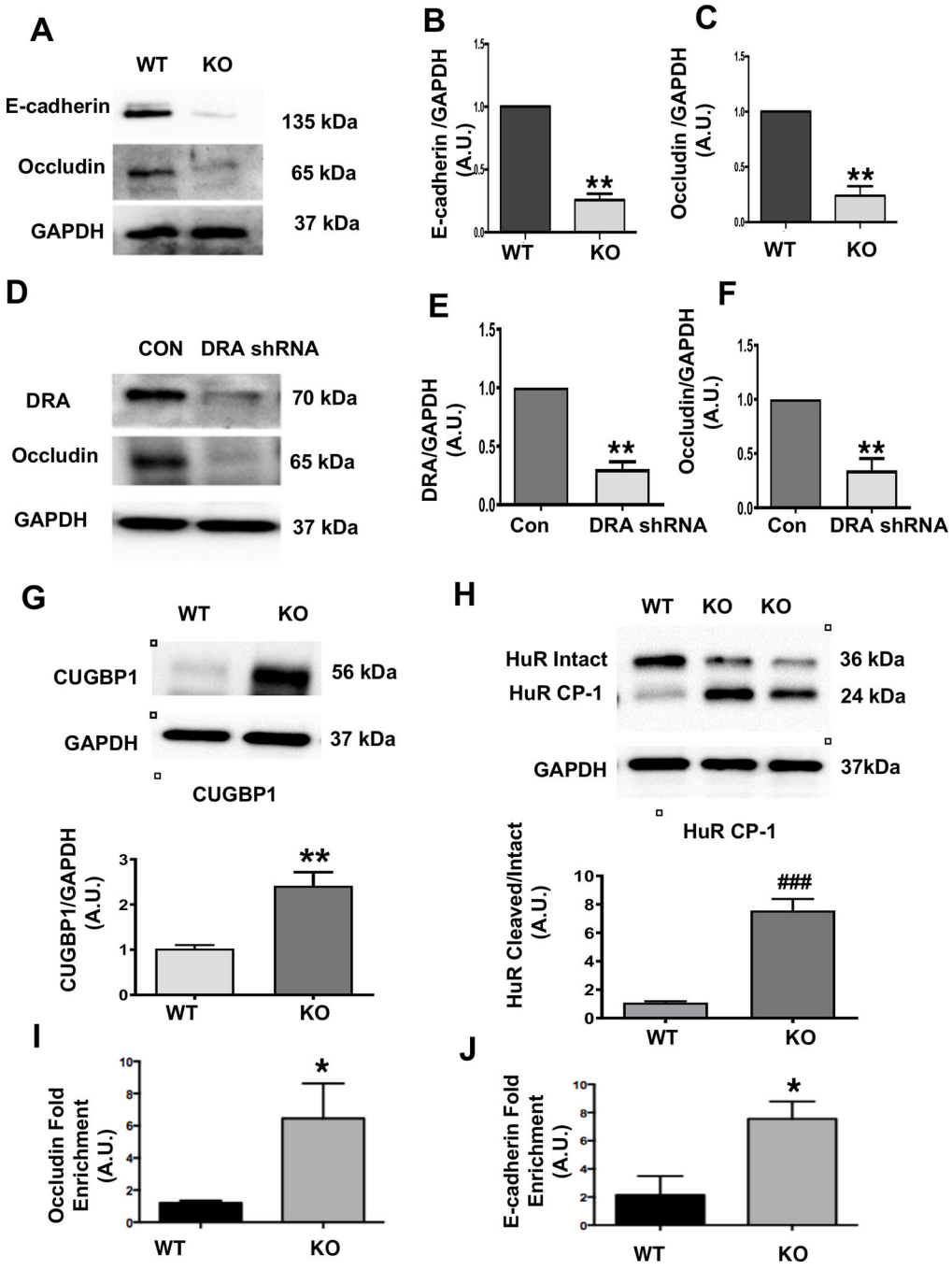

Figure 4: Loss of DRA results in reduced TJ/AJ protein expression in colonoids and Caco-2 cells and increased CUGBP1 expression, HuR protein cleavage, and binding of CUBGP1 to 3' UTR of occludin and E-cadherin in DRA KO mice:

Protein expression of E-cadherin and occludin in colonoids from wild type and DRA KO mice by western blotting **(Figure A).** Densitometric analyses of band intensities (GAPDH was used as the internal control) are shown (**Figures B and C).** DRA and occludin immunoblotting in lentiviral shRNA mediated knockdown of DRA in Caco-2 cells are shown (**Figure D)**. Densitometric analyses of band intensities (GAPDH was used as the internal control) are shown (**Figures E and F).** Values (for figures 4B,4C,4E,4F) are means

± SEM from blots from 3–4 independent experiments. Data was analyzed by unpaired t-test (**p <0.01 vs. wild type). Western blot and densitometric analysis of CUGBP1 and HuR protein levels in distal colonic mucosal lysates of wild type or DRA KO mice (**Figures G and H**). Results represent means ± SEM of 3–4 mice (**p <0.01 compared to wild type, ###p <0.001, cleaved compared with intact HuR). CUGBP1 binding (over IgG) to 3'UTR of occludin and E-cadherin as measured by RNP-IP Assay (**Figures I and J**). Values are means ± SEM of blots of 4–5 independent experiments. Data was analyzed by unpaired t-test (*p <0.05 compared to wild type).

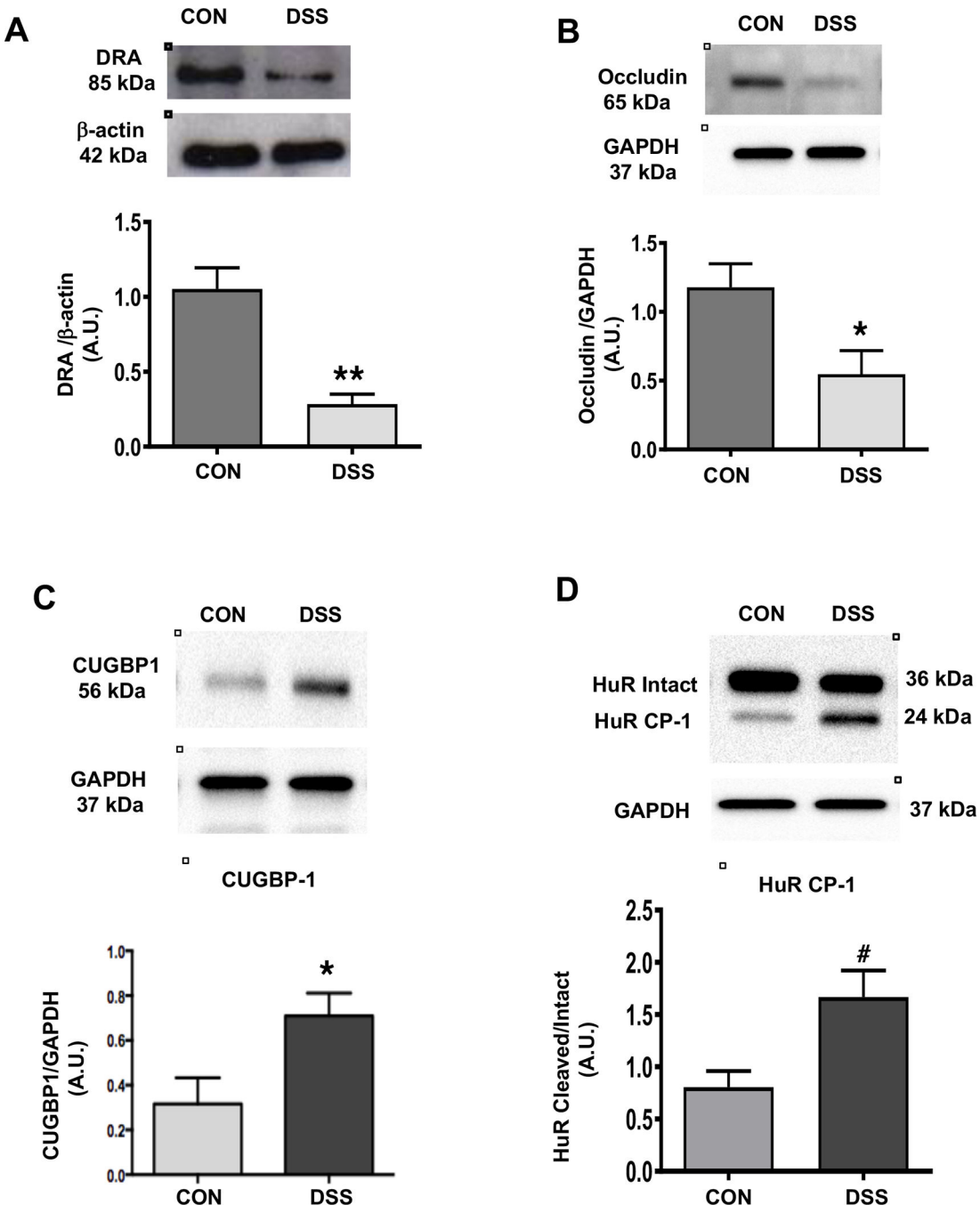

Figures 5: DSS-colitis results in decreased protein levels of DRA, occludin, and increased protein levels of CUGBP1 and cleaved-HuR:

Representative western blots and densitometric analysis of DRA and occludin protein levels in distal colonic mucosal tissue lysates of DSS or control mice (**Figures A and B)**. Results represent means ± SEM of 4 mice. (*p <0.05 and **p <0.01 compared to controls). Representative western blots and densitometric analysis of CUGBP1 and HuR protein (intact and cleaved HuR) levels in distal colonic mucosal tissue lysates of wild type or DRA KO mice (**Figures C and D**). Results represent means ± SEM of 3 mice. Data was analyzed

by unpaired t-test (*p <0.05 CUGBP1 in DSS mice compared to control mice. #p <0.05, cleaved HuR/intact HuR in DSS mice compared to control mice).

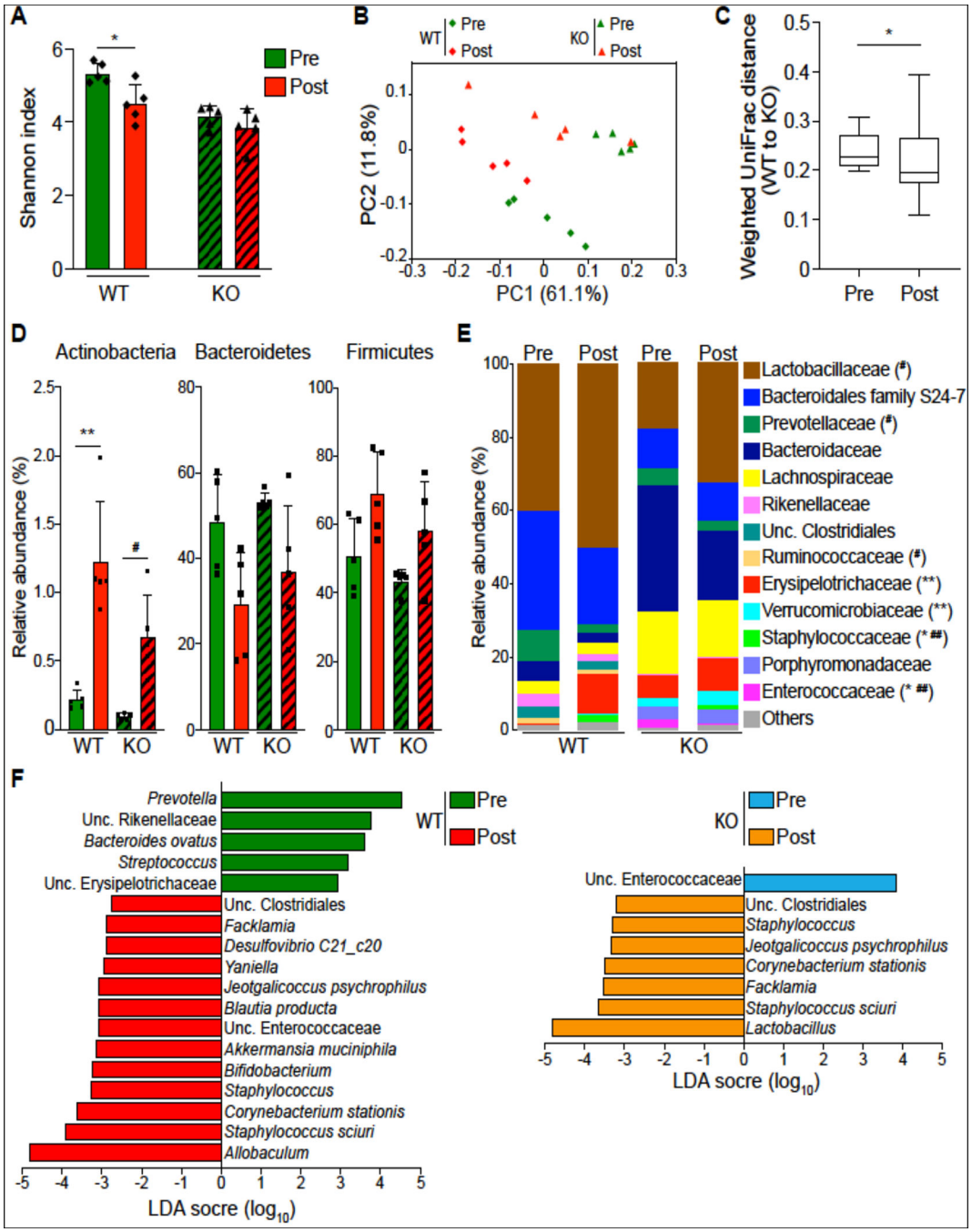

Figure 6. Cohousing contributes to partial exchange of fecal microbiota in DRA KO and WT mice.

Shannon index of fecal microbiota in post-cohoused DRA KO and WT mice compared to their pre-cohoused counterparts (n=5) (**Figure A**). Weighted Unifrac PCoA plot showing community variation in indicated mouse groups (**Figure B**). Weighted Unifrac distances between cohoused mice and their pre-cohoused controls showing the reduced similarity between DRA KO and WT mice after cohousing (**Figure C**). Averaged relative abundances of top phyla (**Figure D**) and families (**Figure E**) in pre- and post-cohoused DRA KO and

WT mice. LEfSe plots showing differentiating taxa (species level) between post-cohoused mice and their pre-cohoused controls (**Figure F**). *p <0.05, **p <0.01, pre-cohoused WT vs. post-cohoused WT; #p <0.05, ##P <0.01, pre-cohoused KO vs. post-cohoused KO.

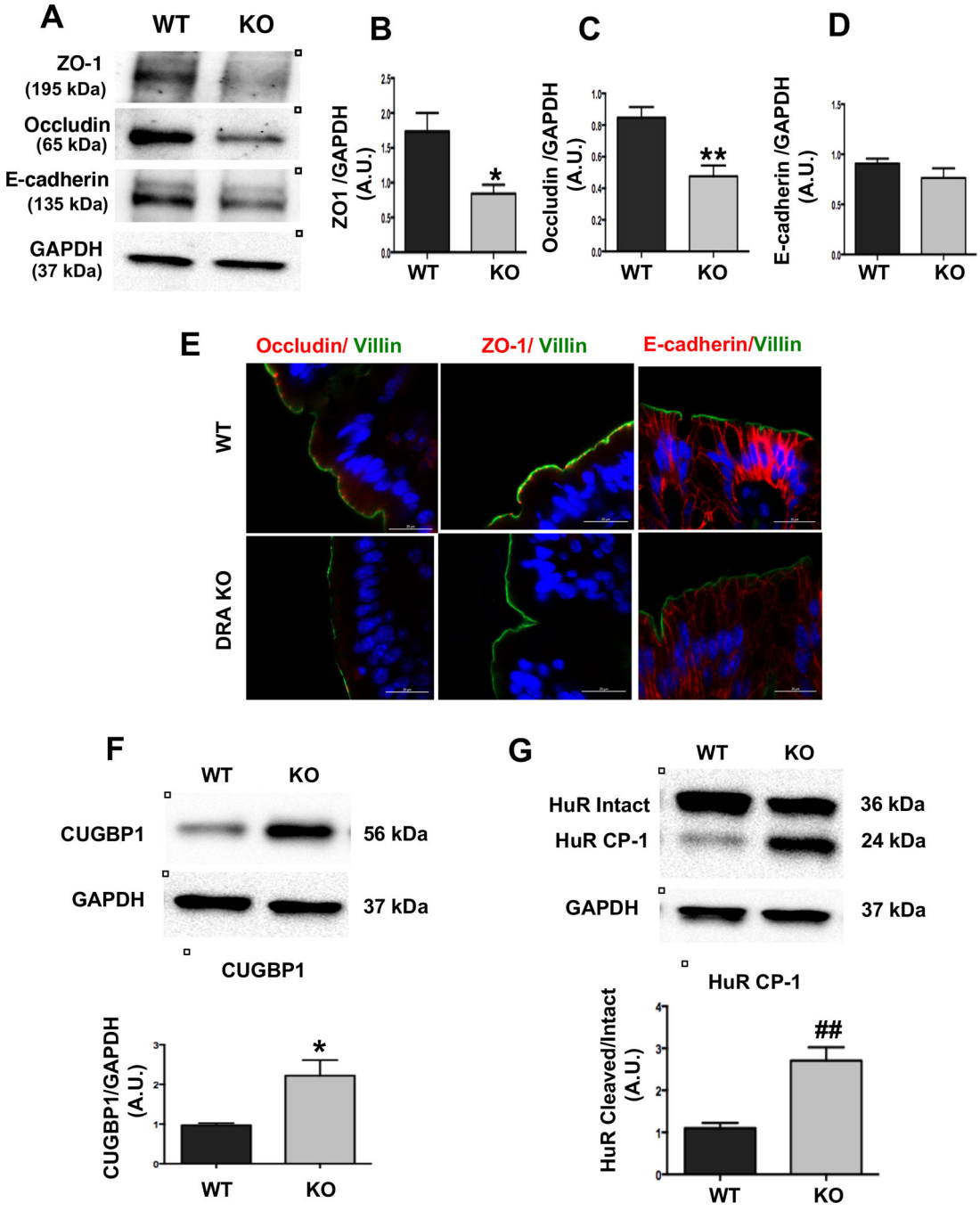

Figure 7: TJ/AJ protein and RBPs expression in cohoused wild type and DRA KO mice:

Protein expression of ZO-1, occludin and E-cadherin in distal colon of wild type and DRA KO co-housed mice (**Figure A**). Densitometric analyses (GAPDH was used as the internal control) of band intensities are shown (**Figures B, C and D).** Values are means ± SEM of blots from 4 wild type and 5 KO co-housed mice. Data was analyzed by unpaired t-test (*p <0.05 vs wild type, **p <0.01 vs. wild type). Immunostaining for ZO-1, occludin, and E-cadherin is shown (**Figure E)**. Scale bar: 20 μm. Protein expression of CUGBP-1 and HuR in distal colon of wild type and DRA KO co-housed mice by western analysis and

densitometric analyses (GAPDH-internal control) of band intensities is shown (**Figures F and G)**. Values are means ± SEM of blots from 4 wild type and 5 KO mice. Data was analyzed by unpaired t-test (*p <0.05 vs wild type, ## p <0.01 vs. wild type).